

# Two-Phase Analysis of Nanofluid Flow Through A Channel With Heat Transfer

Maloth Ganesh

A Thesis Submitted to  
Indian Institute of Technology Hyderabad  
In Partial Fulfillment of the Requirements for  
The Degree of Master of Technology



Department of Mechanical and Aerospace Engineering

June 2019

## Declaration

I declare that this written submission represents my ideas in my own words, and where ideas or words of others have been included, I have adequately cited and referenced the original sources. I also declare that I have adhered to all principles of academic honesty and integrity and have not misrepresented or fabricated or falsified any idea/data/fact/source in my submission. I understand that any violation of the above will be a cause for disciplinary action by the Institute and can also evoke penal action from the sources that have thus not been properly cited, or from whom proper permission has not been taken when needed.

M. Ganesh

(Signature)

Maloth Ganesh

(Maloth Ganesh)

ME17MTECH11023

(Roll No.)

## Approval Sheet

This Thesis entitled Two-Phase Analysis of Nanofluid Flow Through A Channel With Heat Transfer by Maloth Ganesh is approved for the degree of Master of Technology from IIT Hyderabad



( Dr.Narasimha Mangadoddy ) External examiner  
Dept. of Chemical Engineering  
IITH



(Dr.Pankaj Sharadchandra Kolhe) Internal examiner  
Dept.of Mechanical and Aerospace Engineering  
IITH



(Dr.Venkatasubbaiah K) Adviser  
Dept. of Mechanical and Aerospace Engineering  
IITH



(Dr.Narasimha Mangadoddy) Chairman  
Dept. of Chemical Engineering  
IITH

## Acknowledgements

I express my sincere gratitude to my adviser Dr.K.Venkatasubbaiah for his valuable guidance, support and encouragement throughout my work. His interest and confidence in me has helped immensely for the successful completion of this work. I would like to thank all the committee members for their constructive comments and ideas that has boosted my interest in my master project.

I would like to thank Mechanical and Aerospace Department of IITH and the entire IIT Hyderabad system for providing us an excellent computational facility to work upon. I also thank our lab assistant Mr. V Srikanth sir for helping me in any technical issue related to the computational system.

I would like to thank my fellow researchers Neelapu Satish, Abhijith MS, Veeresh Takure and kaveenraj H for their valuable suggestions at various points of the thesis and maintaining friendly environment in the lab.

I would also like to thank all my friends in IIT Hyderabad for making my stay at IIT Hyderabad, memorable and enjoyable.

Finally, I would like to thank my parents for their support, blessings and motivation throughout my work.

# Dedication

To  
My Beloved Family

## Abstract

Nano fluids have great significance towards heat transfer applications. It needs to study the nanofluid flows through channels with heat transfer. A steady an incompressible two dimensional forced convection laminar parallel flow through a microchannel and the effect of impinging plane jet flow in a mini-channel using nanofluids studied numerically. In the present study, nanofluid flows through channels are modeled by using a two-phase approach Eulerian-Eulerian model is used. The present study is valid the Reynolds number up to laminar zone. The governing equations solved by using finite volume schemes with first order implicit for time integration. Studied heat transfer characteristics, the parallel flow through micro-channel  $Re$  from 109.54 to 285.6, observed heat transfer enhancement with 17.63%, studied the effect of volume fraction in heat transfer with the parallel flow and also studied the effect of base fluids that is the kerosene-based fluid has netted more heat transfer than water-based nanofluid. With the jet flow as the Reynolds, number increases average nusselt number also increases, and also observed the effect of volume fractions on the heat transfer at  $Re = 200$ , as the volume fraction from(0.001% to 0.1%) there is an enhancement with 223.23%. Studied the effect of aspect ratios on the heat transfer rate, observed that as the jet inlet to a target surface distance increases average nusselt number decreases. From three different nanofluids ( $H_2O - Al_2O_3$ ,  $H_2O - CuO$ ,  $H_2O - TiO_2$ ) at all volume fractions 0.1%, 1%, 2% the  $H_2O - TiO_2$  has better enhancement in heat transfer. Observed that the velocity and temperature difference between the liquid phase and solid phases is very small and negligible. The present results are matching well with experimental and numerical results available in the literature.

# Contents

Declaration . . . . .	ii
Approval Sheet . . . . .	iii
Acknowledgements . . . . .	iv
Abstract . . . . .	vi
<b>Nomenclature</b>	<b>viii</b>
<b>1 Introduction</b>	<b>1</b>
1.1 Nanofluids . . . . .	1
1.2 Nanofluids with microchannels . . . . .	2
1.3 Jet impingement with nanofluids . . . . .	3
1.4 Literature survey . . . . .	3
1.5 Motivation . . . . .	6
1.6 Objectives of the present study . . . . .	7
1.7 Outline of the thesis . . . . .	7
<b>2 Mathematical formulation with governing equations</b>	<b>9</b>
2.1 Problem definitions . . . . .	9
2.1.1 parallel flow in a microchannel with nanofluids . . . . .	9
2.1.2 Impinging jet flow in a mini-channel with nanofluids . . . . .	9
2.2 Assumptions of the present study . . . . .	10
2.3 Governing equations . . . . .	10
2.3.1 Continuity equations : . . . . .	10
2.3.2 Momentum equations : . . . . .	10
2.3.3 Energy equations : . . . . .	10
2.4 Boundary conditions . . . . .	11
2.4.1 parallel flow in a microchannel . . . . .	11
2.4.2 Boundary conditions of parallel flow through a microchannel: . . . . .	11
2.4.3 Impinging slot jet flow through a mini-channel using nanofluids: . . . . .	11
2.4.4 Boundary conditions of impinging slot jet flow in a mini-channel: . . . . .	12
<b>3 Numerical methods</b>	<b>13</b>
3.1 Openfoam . . . . .	13
3.1.1 Reacting two-phase Euler foam . . . . .	14
3.1.2 Case folders . . . . .	14

3.1.3	solver final details . . . . .	16
3.1.4	Numerical schemes used with OpenFOAM solver . . . . .	17
3.2	Ansys fluent . . . . .	17
3.2.1	Pre processing . . . . .	17
3.2.2	Numerical schemes with Ansys fluent solver . . . . .	20
<b>4</b>	<b>Results of micro-channel flow using nanofluids</b>	<b>21</b>
4.1	Grid Independence test at $Re = 285.86$ . . . . .	21
4.2	velocity and temperature contours, $Re = 285.86$ . . . . .	22
4.3	Validation . . . . .	23
4.3.1	Validation with experimental results . . . . .	23
4.3.2	Validation with single phase approach numerical results . . . . .	24
4.3.3	Effect of Reynolds number . . . . .	25
4.3.4	effect of volume concentration . . . . .	26
4.3.5	effect of base fluids . . . . .	27
<b>5</b>	<b>Results of impinging slot jet flow using nanofluids</b>	<b>29</b>
5.1	Grid independence test . . . . .	29
5.2	Velocity and temperature contours at $Re = 200$ . . . . .	30
5.3	Validation . . . . .	31
5.4	Stream function contours of Dispersed phase(Aluminium oxide particles) . . . . .	33
5.5	Effect of Reynolds number . . . . .	34
5.6	Effect of volume concentration . . . . .	34
5.7	Effect of aspect ratio . . . . .	36
5.8	Effect of nanofluids . . . . .	36
5.9	Velocity profiles of both phases at different locations . . . . .	37
<b>6</b>	<b>Conclusions</b>	<b>40</b>
	<b>References</b>	<b>41</b>



# List of Figures

1.1	impact of nano technology on industrial sector[1]	2
1.2	comparisons of thermal conductivity of various materials [2]	2
2.1	microchannel	9
2.2	impinging slot jets flow	10
3.1	fluent solver settings	18
3.2	solver settings	19
4.1	water U velocity profile with height of the channel	21
4.2	Water Temperature profile with different grids along the H of the channel	22
4.3	U velocity of water	22
4.4	Water Temperature along the height of the channel	23
4.5	$NU_{avg}$ vs $RE$	25
4.6	$NU_{avg}$ vs $RE$	26
4.7	Length vs mean tempararure	27
4.8	Length vs $NU_{local}$	27
5.1	horizontal velocity of water L vs H	29
5.2	horizontal velocity of water L vs H	30
5.3	Velocity contour of water L vs H	30
5.4	Temperature contour of water L vs H	31
5.5	local nusselt number variation along L	32
5.6	local nusselt number variation along L	32
5.7	Stream function contour at $RE=100$	33
5.8	Stream function contour at $RE=200$	33
5.9	Stream function contour at $RE=300$	33
5.10	$NU_{avg}$ with Reynolds number	34
5.11	heat transfer coefficient along L	35
5.12	$NU_{avg}$ vs $\phi$	35
5.13	vertical inlet velocity along H	38
5.14	vertical velocity along Height of the channel	38
5.15	U velocity along Height of the channel	39

# List of Tables

3.1	Type of boundary in openfoam. . . . .	15
3.2	openfoam solver schemes. . . . .	17
3.3	ansys fluent solver schemes . . . . .	20
4.1	code validation . . . . .	24
4.2	code validation with single phase approach . . . . .	24
4.3	average nusselt number variation with $\phi$ % . . . . .	26
4.4	average nusselt number variation with basefluids . . . . .	28
5.1	average nusselt number variation with aspect ratio . . . . .	36
5.2	effect of nanofluids . . . . .	37

# Nomenclature

$NU_{avg}$	Average nusselt number
$Re$	Reynolds number
$\epsilon_l$	Volume fraction of liquid phase
$\epsilon_s$	Volume fraction of solid phase
$\mu_l$	Dynamic viscosity of liquid phase ( $Ns/m^2$ )
$\mu_s$	Dynamic viscosity of solid phase ( $Ns/m^2$ )
$\phi$	Volume concentration
$\rho_l$	Density of the liquid phase ( $kg/m^3$ )
$\rho_s$	Density of the solid phase ( $kg/m^3$ )
$C_{pl}$	Specific heat of liquid phase ( $J/kgK$ )
$C_{ps}$	Specific heat of solid phase ( $J/kgK$ )
$d_p$	Diameter of particle (m)
$F_{drag}$	Drag force ( $N$ )
$K_l$	Thermal conductivity of liquid phase
$K_s$	Thermal conductivity of Solid phase phase
$T_i$	Inlet temperature (K)
$T_l$	liquid phase temperature (K)
$T_s$	Solid phase temperature (K)
$T_w$	wall temperature (m)
$u, v$	Velocity components in x and y directions
$u_i, v_i$	Inlet velocity components in x and y directions
$v_l$	velocity of liquid phase (m/s)
$v_s$	velocity of Solid phase (m/s)

$X, Y$	Dimensionless scales in x and y directions
$x, y$	Cartesian co-ordinates
H	Height of the channel (m)
L	Length of the channel (m)
W	Width of Jet (m)

# Chapter 1

## Introduction

### 1.1 Nanofluids

Basically, nanofluids are the suspensions of nanoparticles in a base fluid. The term nano-particle has come from the Latin prefix nano, it is denoted by  $10^{-9}$  part of a unit. Generally, the nano-term used to denote the size of any unit. First-time nanofluids are introduced by the Choi and Eastman in 1995[1], nanofluids are engineered colloidal suspension of nanoparticles into the base fluid, typically the water is taken as the base fluid. Nanofluids are generally considered the size of particles from (1-100nm) suspended in the base fluids. Nanofluids in the heat transfer applications having their own differences from the conventional fluids like solid-liquid suspensions. Nanofluids consists of a lot of advantages[2]over the other conventional fluids.

#### **Advantages:**

- Having high surface area because of this there is more surface heat transfer between particles and fluid.
- High dispersion stability with Brownian motion of particles.
- For same heat transfer intensity the required pumping power with nanofluid is less than the pure liquid.
- Thermal conductivity of nanofluids will increases with nano-particles, with variable concentrations and maintaining good surface wettability so nanofluids can be used for many other applications.

Nanofluids can be used for a lot of applications, now a days nanofluids can be used for more variety in industries, transportation,energy production and in micro-electro-mechanical systems as well as in electronics systems like in microprocessors.these are also used in biotechnology field,in cooling of automobile engines,to cool welding equipments in less time and also for the cooling of high powered microwave tubes and laser diode arrays. Nano-technology has a great impact on the future.

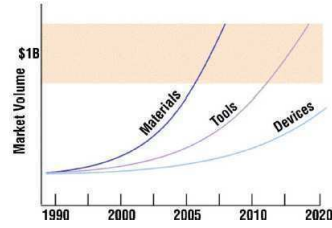


Figure 1.1: impact of nano technology on industrial sector[1]

The figure 1.1 shows the nanotechnology in various sectors usage [1].

The thermal conductivity of nanofluids have more importance towards the usage of materials, because the selection of material also the main thing to form good nanofluid, that means the nanoparticles thermal conductivity should be more, it has been proved that the thermal conductivity of nanofluids have more thermal conductivity than base fluids.

The thermal conductivity of nanofluids depends on particle concentration, as the particle concentration increases the thermal conductivity of nanofluids also increases, it also depends on the particle temperature, size of the particle. The stability and dispersion of particles also main things to define the thermal conductivity of the nanofluids.

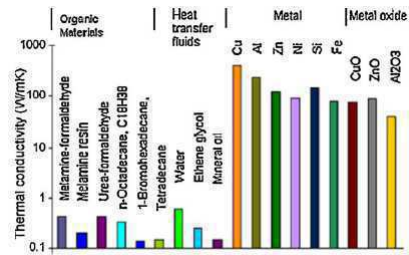


Figure 1.2: comparisons of thermal conductivity of various materials [2]

from figure 1.2 shows that the thermal conductivity of metals is high compared to metal oxides, organic materials, and heat transfer base fluids. it shows that if we choose the nanoparticles with metals there will be high thermal conductivity, which is dispersed into base fluids like water, ethylene glycol, and mineral oil, etc. From figure1.2 it also shows that the thermal conductivity of copper is highest so in most of the applications copper and aluminum metals have been used as nanoparticles for better heat transfer rate which are dispersed into heat transfer fluids.

## 1.2 Nanofluids with microchannels

The study of heat transfer by using nanofluids is so much attracted because we can use these nanofluids in a various phenomenon in equipment. Nowadays nanofluids have so much significance with flow through microchannels. The first time the usage of nanofluids [3] that is the dispersion of mini-sized particles into the liquids to achieve enhanced thermal properties, he explains was failed due to large mass particles and formation of sedimentation then after that Choi et.al [4] introduced

new heat transfer fluids are nanofluids.

Microchannels were introduced by Tuckerman and Pease [5] both were designed and tested a small and compact which is used for water-cooled heat transfer sink for a silicon circuit. So far we have many industrial applications by using microchannels such as in microelectronic cooling that is cooling of microchips processors, To exchange the heat transfer from one fluid to other fluid i.e. in industrial heat exchangers, in automotive to cool the engines, renewable energies like in solar collectors to absorb the heat from the sun rays that to transfer for usage, microchannels also used in nuclear reactors etc..

### 1.3 Jet impingement with nanofluids

The jet impingement is the flow in the form of a jet which is vertical impingement in a channel. The jet impingement is playing an important role in heat transfer phenomenon in channel flows and this Impinging jet has many industrial applications [6], the jet flows with nanofluids will provide the localized high heat transfer coefficients, because of the above reasons these impinging jets are mostly applied to drying of textiles, film paper, to cool efficiently in less time, the very high temperature containing gas turbine blades, also to freezing of tissue in cryosurgery, this jet impingement also applied in manufacturing and material processing and also applied to electronic cooling. The jet impingement in a channel generally constant wall temperature, constant heat flux mostly used at bottom of the channel. The advantage of using jet impingement with nanofluids to increase the heat transfer rate with nano-particles concentrations.

As the flow is vertical impingement on the bottom surface and the particles size is in nano, thereby surface area is small hence localized heat transfer coefficients of nanofluid will increase by this heat transfer rate will increase, Jet impingement is also can be circular slot, plane slot, with single or double jet it depends on application in heat transfer problems and also the flow can be laminar, turbulent it depends on the applications.

### 1.4 Literature survey

Studies have been done using a single phase method (homogenous method) modeling for nanofluid. Koo and Kleinstreuer [7] both of them studied that the laminar flow through a microchannel with single phase approach mixture of copper oxide nano-spheres dispersed into the water, ethylene glycol at low volume concentrations and they used large and higher Prandtl number carrier fluids, nanoparticles at higher concentrations above 4%. Lelea et.al [8] this paper belongs to both numerical and experimental the flow through a microtube, Reynolds number range upto 800, reported that with different tube diameters 0.1, 0.3, 0.5 mm for this cases they compared the experimental results with theoretical as well as with numerical modeling, water is taken as the working fluid. the cooling performance using a microchannel heat sink, the both Jang and Choi [9] using nanofluids copper 6nm in water and 2nm in water studied numerically. the heat transfer enhancement in turbulent tube flow [10] using aluminum oxide nanoparticles studied numerically, in this paper, they have shown that due to the increase of concentrations that affected the wall shear stress increases drastically. the thermal performance of nanofluids studied by Li and Kleinstreuer [11] they have reported with the use of  $CuO$ -water nanofluids from volume fractions 1% to 4% with  $d_p=28.6\text{nm}$  in microchannel mixture

flow the thermal performance increases with a small increment in pumping power. santra et.al[12] they studied the laminar flow through two isothermally heated plates using copper-water nanofluid, they reported that as the Reynolds number from(5-1500) and volume fractions(0.00 to 0.050) the rate of heat transfer increases. The experimental studies had performed by Wu et.al[13]with single-phase flow and heat transfer characteristics in a trapezoidal microchannel with water-aluminum oxide nanofluid, volume fractions are 0,0.15%,0.26%, they showed with experiments the pressure drop and flow friction is slightly higher for nanofluids compare to pure water,there is deposition of this  $Al_2O_3$  particles on the inner walls of microchannel as the temperature of wall increases.

Bianco et.al[14]the laminar flow through a circular tube using water- $Al_2O_3$  nanofluid, constant uniform heat flux applied at the wall numerically studied, shown that maximum average heat transfer coefficient difference between single-phase and two-phase models about 11%, convective heat transfer coefficient for nanofluids is more than that of base fluids. Lotfi et.al[15] they studied that aluminum oxide-water nanofluid flow through the horizontal tubes with forced convection numerically, they also reported that the mixture model is more precise than eulerian-eulerian and single phase methods and also shown that effect of concentrations on the thermal parameters. Ford et.al[16] studied the nanofluid heat transfer considered in a tube with a single phase and two-phase methods and reported that with 0.2% concentration Cu-water nanofluid. they observed that relative error is 16% between the experimental data and single phase model while the two-phase method is 8%. Recently studied that, Kalteh et.al[17] used a EulerianEulerian two-fluid model to study heat transfer inside a microchannel.they considered the probable velocity and temperature difference between phases in their model. and they showed that in their results single phase model underestimate the average Nusselt numbers for nanofluids.there are many experimental studies for nanofluids in macro and micro scales studied by wu.et al[13]they had investigated the heat transfer with water- $Al_2O_3$  nanofluid in the entrance region of copper tube with a diameter 4.5mm,the tube applied with the constant heat flux conditions.after that they observed that their measurements showed that the heat transfer is more especially at the entrance region.

Heris et.al[18], they had compared experimental results with single phase(homogeneous) model, observed that there is underestimate in heat transfer with a single phase model especially at higher volume concentrations. the laminar forced convection heat transfer of an aluminum oxide-water nanofluid inside an isothermally heated circular tube is studied experimentally[19]. In this, they obtained the nusselt numbers for different Reynolds numbers and pecllet numbers, the nusselt numbers of nanofluids more than the single phase results and also shown that heat transfer increases by increasing concentrations of particles.Izadi et.al[20]performed the numerical investigation on forced convection flow in a microscale duct using nanofluids they observed that the effect of volume concentrations on heat transfer at the thicker wall is more efficient. Jung et al.[21] they did experiments over  $Al_2O_3$ -water nanofluids in a rectangular microchannel, they considered the particle diameter is 170 nm, with only 1.8% particle concentration there is 32% increase in heat transfer coefficient in compared to single phase distilled water.

kalteh[22], investigated the effect of various nanoparticle and base liquid types on the nanofluids flow in a microchannel, used EulerianEulerian two-phase approach, compared the different



nanoparticles( $Al_2O_3$ ,  $Sio_2$ ,Diamond etc) and different base fluids ( water,ethylene glycol etc.), they also observed that heat transfer performance of diamond in water nanofluid was found better than the rest of the nanofluids.Kalteh et.al[23] this is an experimental investigation used eulerian-eulerian model for modeling nanofluid flows in microchannels, reported that for the laminar flow aluminum oxide-water nanofluid the two-phase method is better than the homogenous method to predict the heat transfer experimentally and two-phase results are showing that velocity and temperature between two-phases is very small and negligible. Rajesh and Venkata subbaiah[24]both of them investigated the conjugate performance, laminar forced convection flow in a microchannel using different nanofluids  $Al_2O_3$ -water, silver,silver+ $Al_2O_3$  hybrid nanofluids used,it is a single-phase approach,reported that at 3% volume concentration of  $Al_2O_3$ -water nanofluid the heat transfer enhances by 17% to 18% than pure water, by increasing Reynolds number inlet velocity increases with this average heat transfer coefficient increases and the interface temperature between solid and liquid decreases.

Rajesh and Venkatasubbaiah[25], they considered single phase approach, they had shown that the gold nanofluids with particle size less than 90 nm is preferable for enhancing heat transfer at volume concentration 2%, at Reynolds number = 400, the enhancement varies from 41% to 90% for gold nanofluid with diameter particle 30 nm while particle concentration ranging from 1.0 vol% to 3.0 vol%. experimental and multiphase analysis of the nanofluids on the conjugate performance of microchannel at low Reynolds numbers[26], they used two-phase mixture model approach, at  $Re=50$ , 3% volume concentration *SWCNT* nanofluids enhance the heat transfer by 35.37% in comparison with deionized water for the input of heat flux  $19,658w/m^2$ . and they have shown that there is decreasing in the nusselt number due to the dominating effect of thermal conduction at the solid walls of the microchannel at low Reynold number. Thermal and hydraulic analysis of rectangular microchannel with gallium copper oxide nano-suspension by Sarfraz et.al[27], they performed the experiments over the base fluid gallium and dispersed particles copper oxide nano-suspension, at Cu wt 10% the maximum heat transfer coefficient is achieved whereas wt 15% due to agglomeration of nanoparticles, the viscosity of gallium, heat transfer is decreased.high pressure drop was also reported in case of gallium nanosuspensions in comparison with water and pure gallium.

Convective heat transfer analysis of refined kerosene with alumina particles for rocketry applications, sundaraj et.al[28], performed experimental study on kerosene base fluid with aluminium oxide nanoparticles with low volume concentrations ranging from (0.01% to 0.05%), observed that as the nanoparticle concentration increases from 0.01 to 0.05% there is 16.3% increment in heat transfer.heat transfer in the confined slot jet flow at the low Reynolds number by Lee et.al[29]  $Re=50$  to 500 and with different height ratio from 2-5.they observed that the above critical Reynolds number the thermal field and flow become time-dependent and asymmetric and flow become more complex as the unsteadiness increases.at the unsteady region the  $NU_{avg}$  due to flap motion of the jet flow. Zhou and Lee [30] both studied the forced convective heat transfer using air impinging jet on a heated flat plate experimentally, studied the effects of jet Reynolds number, nozzle to plate distance both local and average nusselt numbers. experimental data correlated and compared with existing previous results in the turbulent flow. Palm et.al[31]the study is about the nanoparticles suspension in radial flow cooling systems numerically investigated, the flow is laminar forced convection flow

between two co-axial parallel disks with central axial injection of this nanofluid (water- $Al_2O_3$ ), it is a single phase approach, they observed by radial flow at low volume fractions at 4% thereby enhancing 25% increase in heat transfer coefficient compared to pure base fluid water. The natural convective boundary layer flow [32] using nanofluid past a vertical plate is studied analytically, used a model which include both Brownian motion and thermospheric by considering simplest boundary conditions at the wall, similarity solutions obtained by using different non dimensional number like Prandtl number  $Pr$ , Lewis number etc. laminar impinging jet on a flat plate with layer of porous material investigated by Dorea et.al [33], this is a numerical study with non equilibrium models, studied effects of porosity, permeability, ratio of fluid to solid thermal conductivity, reported that LNTE model is more advantageous for highly porous material and layer of highly conducting which attached to the cooling wall and for the high solid to fluid thermal conductivity ratio the temperature of the solid phase increases, and the boundary layer at the wall become thicker. by Lamraoui et.al [34], they investigated numerically the thermal and dynamic fluid behavior on Newtonian as well on Non Newtonian fluid using  $Al_2O_3$  water nanofluid with single phase approach in a confined slot impinging jet, a jet Reynold number considered from  $Re$  25 to 300 and particles volume fraction considered from 0 to 5%, they reported that local nusselt number gradually decreases from the stagnation point of targeted surface to outlet section of the channel, the local nusselt number at the symmetry at  $x=0$ , is highest and as the distance increase from the center of axis nusselt number decreases due to decrease in local convection phenomenon with  $Re$ , observed that at same value of  $Re$  the local nusselt number is more for Non Newtonian fluid then Newtonian fluid for the entire target surface, At jet axis  $x = 0$ , a relative increase of 9.8% in heat transfer At  $\phi = 5\%$ ,  $Re = 300$ , whereas the comparison shows at  $\phi=1\%$   $Re = 25$  more significant improvement up to 22%.

They also stated that At same  $Re$ ,  $\phi$  as the increases in the aspect ratio there is a decrease in the local nusselt number due to the effect of the wall to jet inlet distance, as this distance increases the effect of fluid temperature on wall decreases thereby nusselt number is decreasing. Delorenzo et.al [35], these people studied on numerical study of laminar flow in confined impinging slot jets with the nanofluids. it is a single approach problem which is solved numerically, they observed that the local heat transfer coefficient and nusselt number values are highest at stagnation point i.e. (where impinging going to happen) as we increase in volume concentration as well as Reynolds number. They also observed that the maximum increase in heat transfer coefficient at  $\phi = 5\%$  and for the aspect ratio  $\frac{H}{W} = 8$  is 32%. by using this approach required pumping power is increased as well as Reynolds number and Volume concentration these are nearly 3.9 times greater than the values which are calculated for the water.

## 1.5 Motivation

Studies in the past have not much emphasized with two-phase approach Eulerian-Eulerian model, in the literature there are fewer studies have been done using this model, flow through a microchannel with the use of nanofluids numerically. and also in literature few studies have done with impinging slot jets flow in channels, with use of nanofluids by two-phase approach numerically.

### A. Eulerian Eulerian two-phase model

- In the literature, the convective heat transfer with nanofluids modeled using two approaches.
- Single phase approach.
- Two-phase approach.
- Eulerian-Eulerian model uses a two-phase approach.
- In this model assumes both phases to be an interpenetrating continuum.
- In this model, the continuity, momentum, energy equations are solved separately for each phase.

This two-phase approach Eulerian-Eulerian model with nanofluid flows in a channel in the literature fewer studies have been done, so there has been the motivation to the present investigation.

## 1.6 Objectives of the present study

The objective of the present study is to understand the flow and enhancement of heat transfer in an incompressible laminar flow in a two dimensional rectangular microchannel, parallel flow with using nanofluids, the effect of Impinging slot jets flow using nanofluids in a rectangular minichannel in the laminar region.

The objectives of the present study summarized as follows.

- To study the effect of Reynolds number in a microchannel with parallel flow
- To study the effect of volume concentration with the parallel flow in a microchannel
- To study the effect of base fluids in parallel flow
- To study the effect of Reynolds number with impinging slot jets flow in a mini-channel.
- To study the effect of aspect ratio to the heat transfer in the jet flow in a mini-channel.
- To study the effect of volume concentrations with impingement.
- To study the heat transfer by using different nanofluids with the impingement.

## 1.7 Outline of the thesis

Two-phase approach nanofluid flows analysis in channels with heat transfer using parallel and Jet Flows.

- Chapter 1 deals with an introduction to nanofluids with microchannel, jet impingement, literature survey for the present investigation followed by the motivation of the present study.
- Chapter 2 deals with the problem formulation with governing equations, boundary conditions.
- Chapter 3 deals with numerical methods and about the solvers.
- Chapter 4 deals with Results of a microchannel with the use of nanofluids

- Chapter 5 deals with Results of impinging slot jets flow with the use of nanofluids
- Chapter 6 shows about conclusions

## Chapter 2

# Mathematical formulation with governing equations

### 2.1 Problem definitions

#### 2.1.1 parallel flow in a microchannel with nanofluids

To study the enhancement of heat transfer using Eulerian-Eulerian two-phase model, in two-dimensional an incompressible laminar flow through a rectangular microchannel with nanofluids.

The geometry details are taken from kalteh et.al[22] paper.

Height of the channel  $H=0.58\text{mm}$ , length of the channel= $50\text{mm}$ .

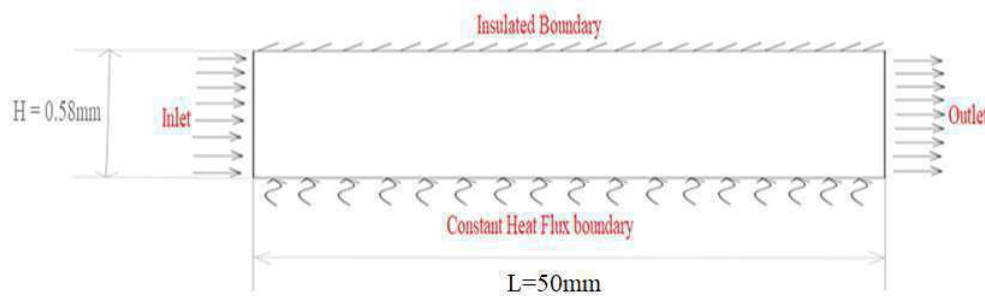


Figure 2.1: microchannel

#### 2.1.2 Impinging jet flow in a mini-channel with nanofluids

To study the enhancement of heat transfer using Eulerian-Eulerian two-phase model, in a two-dimensional an incompressible impinging jet laminar flow through a channel with nanofluids.

the channel details all are taken from the lamraoui et.al[34]paper, the width of jet is  $W=6.2\text{mm}$ ,  $L=62\text{mm}$ ,  $H=24.8\text{mm}$

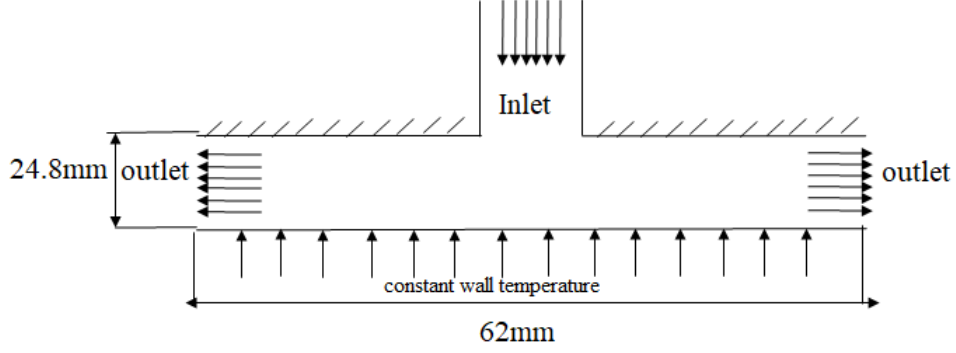


Figure 2.2: impinging slot jets flow

## 2.2 Assumptions of the present study

- The flow is an incompressible
- In laminar region
- At steady state condition
- Two-dimensional

## 2.3 Governing equations

The two-phase Eulerian-Eulerian model considered for modelling the nanofluid flows through channels the equations 2.3.1, 2.3.2, 2.3.3 Eulerian-Eulerian equations for laminar case.

### 2.3.1 Continuity equations :

$$\frac{\partial}{\partial t}(\epsilon_l \rho_l) + \nabla \cdot (\epsilon_l \rho_l \vec{v}_l) \quad (2.1)$$

$$\frac{\partial}{\partial t}(\epsilon_s \rho_s) + \nabla \cdot (\epsilon_s \rho_s \vec{v}_s) \quad (2.2)$$

### 2.3.2 Momentum equations :

$$\frac{\partial}{\partial t}(\epsilon_l \rho_l \vec{v}_l) + \nabla \cdot (\epsilon_l \rho_l \vec{v}_l \vec{v}_l) = -\epsilon_l \nabla p + \nabla \cdot [\epsilon_l \mu_l (\nabla \vec{v}_l) + \nabla \vec{v}_l^T] + \epsilon_l \rho_l g - F_{Drag} \quad (2.3)$$

$$\frac{\partial}{\partial t}(\epsilon_s \rho_s \vec{v}_s) + \nabla \cdot (\epsilon_s \rho_s \vec{v}_s \vec{v}_s) = -\epsilon_s \nabla p + \nabla \cdot [\epsilon_s \mu_s (\nabla \vec{v}_s) + \nabla \vec{v}_s^T] + \epsilon_s \rho_s g + F_{Drag} \quad (2.4)$$

### 2.3.3 Energy equations :

$$\frac{\partial}{\partial t}(\epsilon_l c_{pl} T_l) + \nabla \cdot (\epsilon_l c_{pl} T_l v_l) = \nabla \cdot (\epsilon_l k_{l,l} \nabla T_l) \quad (2.5)$$

$$\frac{\partial}{\partial t}(\epsilon_s c_{ps} T_s) + \nabla \cdot (\epsilon_s c_{ps} T_s v_s) = \nabla \cdot (\epsilon_s k_{s,s} \nabla T_s) \quad (2.6)$$

For the liquid-particle two-phase flow, the relationship between liquid and particle volume fraction is:

$$\epsilon_l + \epsilon_s = 1. \quad (2.7)$$

where  $l$  represents the liquid phase and  $s$  represents the solid phase

## 2.4 Boundary conditions

### 2.4.1 parallel flow in a microchannel

In the case of parallel flow in a microchannel using nanofluid water and aluminum oxide particles for the parallel flow, the uniform velocity and temperature are specified at the inlet of the channel. No slip boundary condition applied on the walls of the channel, at the outlet section of the channel, the fully developed flow condition is assumed for both velocity and temperature fields. the top wall of the channel is considered insulated and adiabatic boundary condition applied to it. Where the bottom wall of the channel is applied with constant wall temperature boundary conditions.

### 2.4.2 Boundary conditions of parallel flow through a microchannel:

- At inlet horizontal uniform velocity and Temperature are specified.

$$u = u_i, T = T_i \quad (2.8)$$

- On the top wall of the channel is adiabatic and no-slip boundary conditions applied.

$$u = 0, v = 0, \frac{\partial T}{\partial y} = 0 \quad (2.9)$$

- On the bottom wall of the channel is applied constant wall temperature and no-slip boundary conditions applied to it.

$$T = T_s, u = 0, v = 0 \quad (2.10)$$

- At the outlet of the channel, the fully developed flow boundary conditions are applied for both velocity and temperature fields.

$$\frac{\partial u}{\partial x} = 0, \frac{\partial T}{\partial x} = 0 \quad (2.11)$$

### 2.4.3 Impinging slot jet flow through a mini-channel using nanofluids:

The impinging slot jets flow in a mini-channel with use nanofluids for the laminar flow. In this problem the jet inlet is at the center of the channel which is impinging like plane jet, in this case, uniform velocity and temperature is specified at inlet boundary, both left and right outlet section of the channel considered be fully developed flow and whereas top wall is insulated and adiabatic boundary condition is applied. On the bottom wall, constant wall temperature condition is applied. No slip boundary condition applied on the walls of the channel.

#### 2.4.4 Boundary conditions of impinging slot jet flow in a mini-channel:

- At the inlet of the channel uniform vertical velocity and uniform temperature is specified.

$$v = v_i, T = T_i \quad (2.12)$$

- At both left and right outlet of the channel, the fully developed flow boundary conditions are applied for both velocity and temperature fields.

$$\frac{\partial u}{\partial x} = 0, \frac{\partial T}{\partial x} = 0 \quad (2.13)$$

- On the top wall of the channel no-slip boundary condition is applied, the wall is insulated and adiabatic boundary condition applied for temperature field.

$$u = 0, v = 0, \frac{\partial T}{\partial y} = 0 \quad (2.14)$$

- On the bottom wall of the channel is applied constant wall temperature and no-slip boundary conditions applied.

$$T = T_w, u = 0, v = 0 \quad (2.15)$$



# Chapter 3

## Numerical methods

To solve the two-phase Eulerian-Eulerian model laminar flow governing equations 2.3.1, 2.3.2, 2.3.3 the relevant software are chosen like OpenFOAM, Ansys fluent etc.

### 3.1 Openfoam

OpenFOAM is free and it is open source as CFD toolbox and OpenFOAM stands for open source field operation and manipulation. There are a lot of advantages over the other software. The advantages are there is no license cost, there are a lot of applications and models are already available to use them, the syntax of all differential equations we can easily understand, according to problem the code can be modified it is user-defined one.

OpenFOAM consists of various solvers, these solvers are in various fields like:

- Incompressible flow solvers with RANS and LES
- Compressible flow solvers with RANS and LES handling capability
- Buoyancy Driven - flow solvers
- Multiphase flow solvers
- Solvers for Combustion Problems
- Solvers for conjugate problems
- Electromagnetic solvers
- Solid dynamic solvers
- Particle Tracking solvers
- Solvers for the DNS and LES

Present for my problem belongs to multiphase flow solver.

### 3.1.1 Reacting two-phase Euler foam

It is a two-phase solver which consists of different phase systems and with different phase, models are available in that they are

Phase systems:

- Heat and Momentum transfer Phase system
  - These system includes both temperature and velocity solving equations for two phases which can be a combination of liquid-solid,liquid-liquid, etc.
- Interface composition Phase change system
  - These systems able to solve problems with different composition with a phase change at the interface.
- Thermal Phase change system
  - This system solves problems like boiling condensations, the temperature of one Phase will change to other phases.

Phase Models: Solver consists of different models

- Pure phase model
  - in this model both phase composition will be the same throughout the simulations, means for example water will be always water, Aluminium particles always remain the same with the composition.
- Reaction phase model
  - with these model we can solve problems like combustions problems for example reaction between oxygen and the fuel, both phases will react to each other and give new composition.
- Isothermal phase model
  - in this model the temperature throught the process is constant, there is no temperature variation in the phases.
- Inert phase model
  - It is for the Phases like noble gases which are stable throught the process.

### 3.1.2 Case folders

#### a. 0

In this Folder we can give the initial conditions of all required properties like temperature, pressure, velocity, concentration etc.

#### b. Constant

In this folder we can define

1. Gravitational acceleration.
2. Phase properties and required phase system: according to our application, we can define the phases and their properties here.
3. Thermo-physical properties we have to define here like density, viscosity, etc.

### c. Polymesh

Here we can define our problem boundary conditions:

For Example, the flow through a rectangular channel with the following boundary conditions defined in OpenFOAM

Table 3.1: Type of boundary in openfoam.

Location	Type of Boundary condition
Inlet	Patch(flow from inlet of the channel)
topwall	Wall
bottomwall	Wall
outlet	Patch(flow from outlet of the channel)

**d. system** In this folder we have sub folders to control the solver

- Controldict
  - It is mainly used for case controls like timing information, write format.
- Start time
  - Here we can give starting time of a case.
- End time
  - End time of case can define here.
- Time step
  - Here we will define the time-step for each iteration for the simulation.
- Latest time
  - It is the time where the simulation will start from the starting of the previous time simulation, so flexible and we can save time with this command in OpenFOAM
- Courant Number
  - which is very important to control the time step for a particular simulation and its maximum value should be the less than unity to prevent the diverging of the solution.
- Fvschemes

- In open foam, the inbuilt code has been developed using the finite volume method, the finite volume method will take every solution in the iteration using cell center value.
- Fvsolution
  - Here we can give tolerances and maximum number of iterations of a particular properties like pressure tolerance  $1e - 07$ .
- DecomposeParadict
  - It is a Command used for divide the mesh for parallel processing i.e. every processor will work separately and give the solution for every time-step
- Fluent.msh
  - These command is used to convert fluent mesh file into Foam mesh.
- Commands used for run the case
  - Of41
  - fluentMeshToFoamMesh
  - DecomposePar
  - mpirun -np -number of parallel processor solver name

### 3.1.3 solver final details

**Solver name:** Reacting two-phase Euler foam

**Type:** In Laminar case

**Phase system:** Heat and Momentum transfer phase system

**Phase model:** Pure phase model ( no reaction within the phases and the composition will not change of a Particular phase

**Diameter model:** Constant (No change in the diameter of the dispersed phase)

**Thermo physical model:** herhothermo, which will use for maintaining the density and temperature of the particular phase at initially is the same,there is no change in temperature of the particular boundary, for example, if we give inlet temperature of a phase like 298 K, density  $999.99kg/m^3$  these quantities remains the same throughout the simulation at inlet

**Dispersed Phase :**  $Al_2O_3$ (Aluminium oxide) particles will dispersed into the base fluid.

**Continuous Phase :** Water.

### 3.1.4 Numerical schemes used with OpenFOAM solver

The OpenFOAM solver code has been developed with the use of the finite volume method, in this method the solution will take the cell center value instead of every node value, to solve governing equations of Eulerian-Eulerian two-phase model the following schemes used as follows, In OpenFOAM all the equations, will be solved with according to their derivative term with corresponding scheme, small time step  $10^{-4}$  is taken to avoid numerical instability.

Table 3.2: openfoam solver schemes.

Derivatives	Used scheme
Time ( $\frac{\partial}{\partial t}, \frac{\partial^2}{\partial t^2}$ )	Euler (Transient, First order implicit)
Gradient( $\nabla$ )	Gauss linear (Linear interpolation or Central differencing, second order)
Divergence( $\nabla \cdot$ )	Gauss linear (second order, bounded)
Laplacian( $\nabla^2$ )	Gauss linear corrected (means linear, second order bounded)

The Eulerian-Eulerian model is a two-phase model having two continuity 2.3.1, two momentum equations 2.3.2 followed by two energy equations 2.3.3, all the terms in the equations for the liquid phase and solid phase solved separately using above schemes.

## 3.2 Ansys fluent

I have not to cope with the OpenFOAM solver to solve impinging of jet flow in a channel, so I have selected Ansys fluent academic version F13.3 to solve my problem.

Fluent software it consists of the broad, physical modeling to handle or to model the flow like turbulence, heat transfer with multiphase systems and other industrial application problems can be solved by fluent.

### 3.2.1 Pre processing

The creation of geometry and meshing is done using academic ICEM CFD 13.0 version, after successful meshing the mesh has to import into Ansys fluent.

All the required input conditions and the solution set up flow chart follows like:

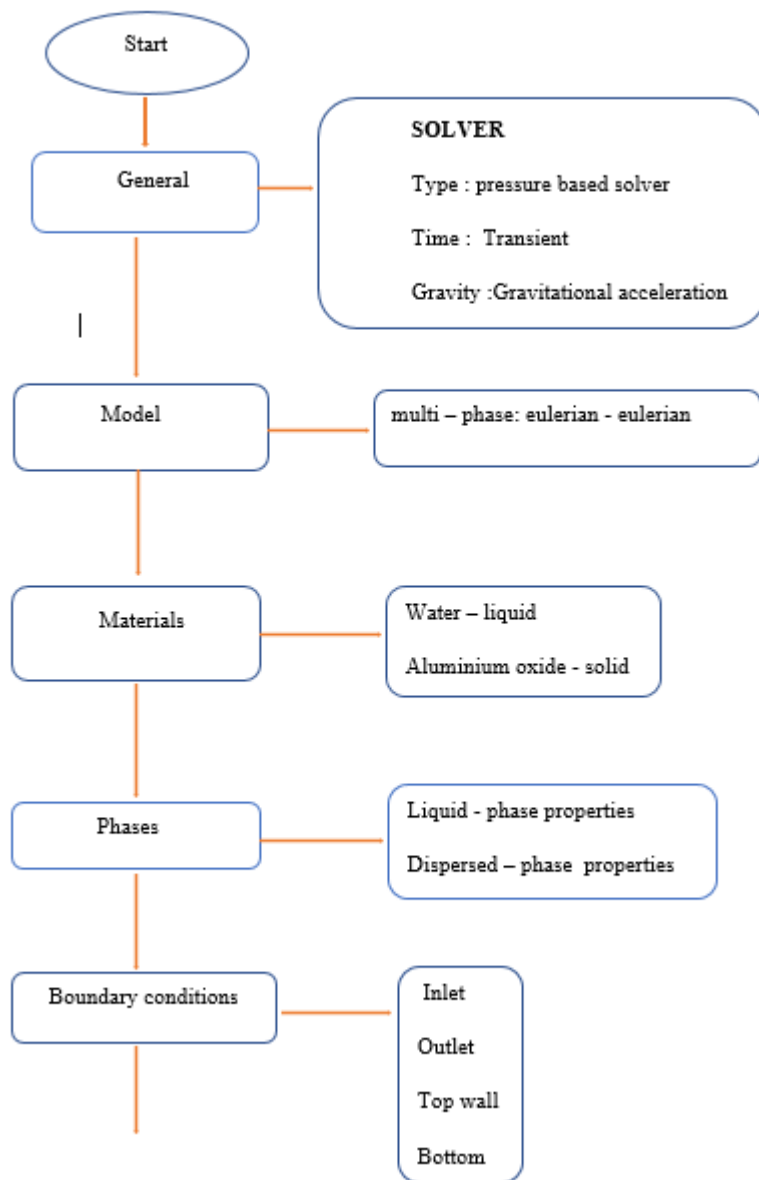


Figure 3.1: fluent solver settings

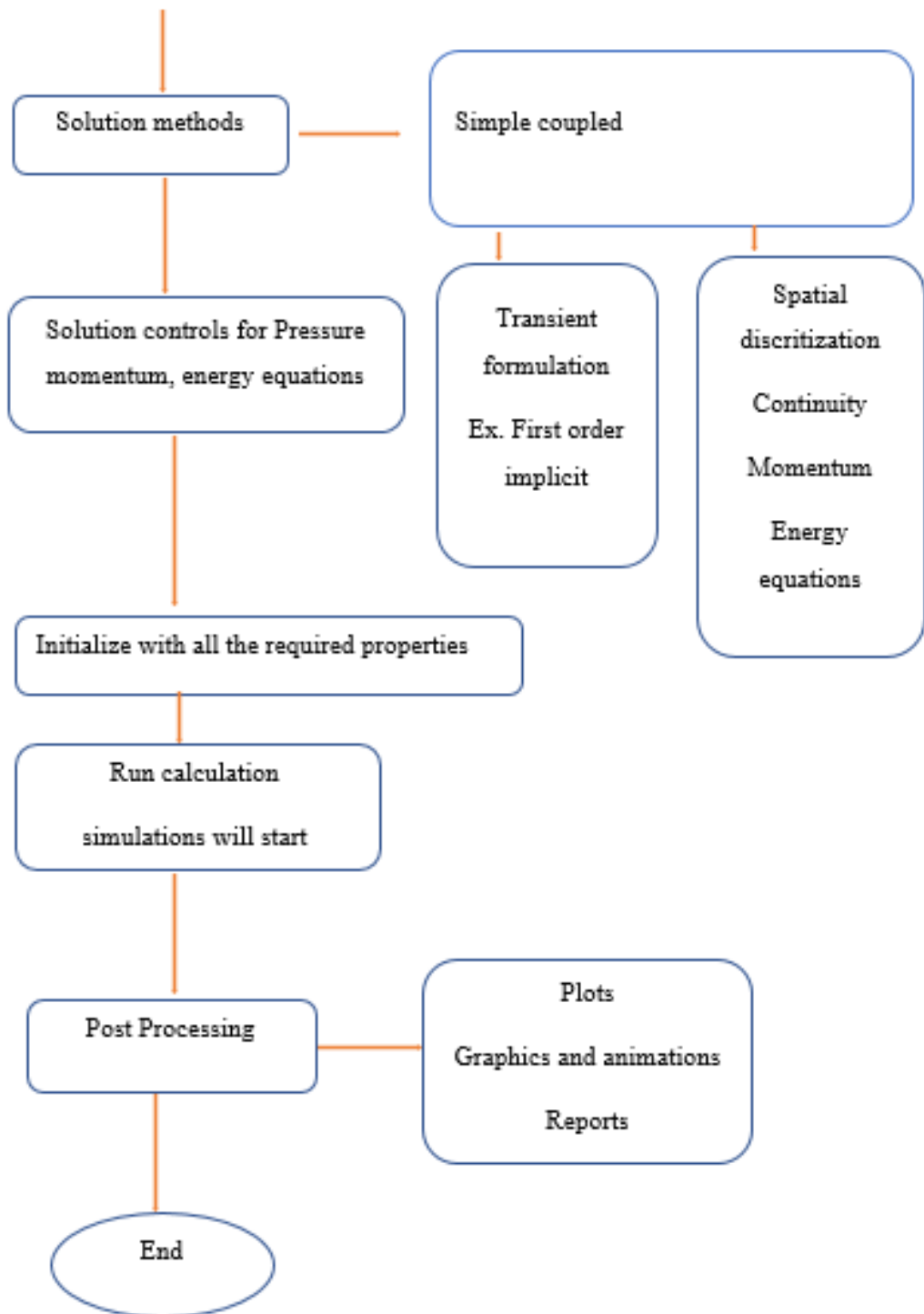


Figure 3.2: solver settings

### 3.2.2 Numerical schemes with Ansys fluent solver

Fluent software also developed inbuilt code with the finite volume method, the convergence solution for every iteration is the cell center value, the Eulerian-Eulerian model is chosen to solve the impinging of slot jets laminar flow with nanofluid in a channel, the simple phase coupled scheme is chosen for the pressure-velocity coupling, smaller time step  $10^{-3}$  is taken to avoid numerical instability.

The Numerical methods are chosen for this problem as follows.

Table 3.3: ansys fluent solver schemes

Transient Formulation ( Time discretization )	First order implicit
Gradient (continuity equations)	Least square cell based
Momentum equations	Second order upwind
Volume fraction	First order upwind
Energy equations	Second order upwind
Pressure velocity coupling	Simple coupled scheme



## Chapter 4

# Results of micro-channel flow using nanofluids

An incompressible laminar flow through a horizontal rectangular microchannel using nanofluids with two-phase approach Eulerian-Eulerian model studied numerically and observed the enhancement in heat transfer with the effect of Reynolds number ( $Re$ ), the effect of volume concentrations and effect of base fluids.

### 4.1 Grid Independence test at $Re = 285.86$

An incompressible laminar flow through a rectangular microchannel using nanofluids with the Eulerian-Eulerian two-phase approach numerically studied, the grid independence test is done with the different grids 200x30,121x15,151x21 at  $Re = 285.86$ , 0.1% volume concentration with  $Al_2O_3$  water nanofluid.

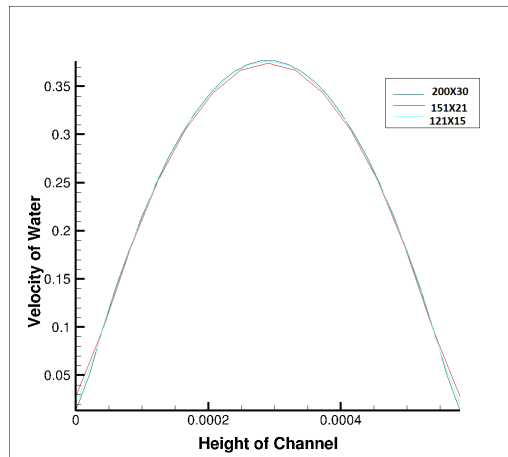


Figure 4.1: water U velocity profile with height of the channel

For the inlet Reynolds number  $Re=285.86$  the velocity inlet is  $0.2520m/s$  from 4.1 at steady state,fully developed condition this velocity is became 1.5 times of the inlet velocity.

Here the maximum velocity of water reached is  $0.369\text{m/s}$  The figure 4.1 shows that there is no change in velocity profiles with the three grids, whereas as the the figure 4.2 represents no changes in temperature profiles of water that means the grid independence is done.

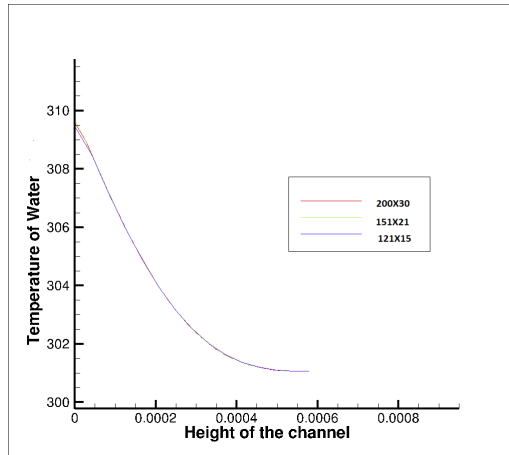


Figure 4.2: Water Temperature profile with different grids along the H of the channel

From the figure 4.2 we can say that at the bottom wall temperature is maximum around 309.9K whereas at the top wall is 301.5K this graph plotted at the outlet section of the channel where the flow is fully developed and at steady state condition. With the three different grids, the temperature profile of water is not changing much that means the water carries the same temperature through the height of the channel, no variation in temperature profile hence grid independence test is done.

## 4.2 velocity and temperature contours, $Re = 285.86$

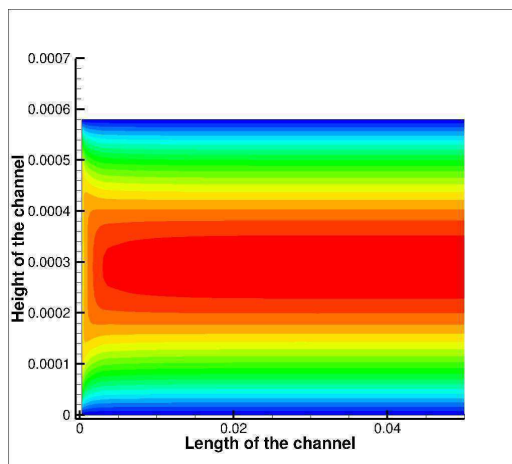


Figure 4.3: U velocity of water

from the above figure 4.3 the flow becomes steady and satisfied fully developed flow. At the center section of the microchannel where the flow velocity is maximum and at the wall of the channel the

velocity is zero to satisfy the no-slip boundary condition. We can see the flow of water in the channel with the streamlines are parallel that means the approximate shape of the velocity profile of water is parabolic.

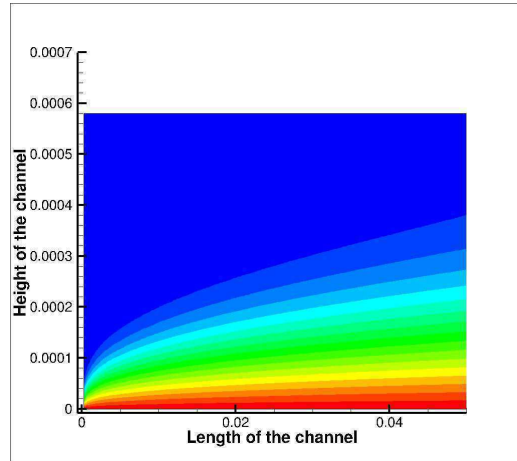


Figure 4.4: Water Temperature along the height of the channel

The figure 4.4 is the temperature contour, at the bottom wall of the channel the constant wall temperature is applied, where as the top wall is insulated. From this 4.4 we can understand that as the height of the channel increases from bottom wall the temperature is decreases. The thermal boundary layer of water increases from inlet to outlet section along the length of the channel due heat taken by fluid is increases.

## 4.3 Validation

### 4.3.1 Validation with experimental results

The validation of solver against the kalteh et.al[23] experimental results that is laminar flow through a microchannel with water and  $Al_2O_3$  nanofluid at  $Re = 285.86$ , 0.1% volume concentration. The constant heat flux of  $20.5k w/m^2$  is applied on the bottom wall of the channel, the size of particles is 40 nm where as the particles viscosity is order of  $1e^{-03}$ [17]

Table 4.1: code validation

Grid size	$NU_{avg}$ kalteh et.al Experimental[23]	$NU_{avg}$ Present	Variation in(%)
121x15	7.710	7.949	3.10
151x21	7.710	7.879	2.191
200x30	7.710	7.8496	1.81

From table 4.1, among these three grids even though 200x30 grid is giving better closed  $NU_{avg}$  compare to other two grids(151x21,121x15) with experimental  $NU_{avg}$  but the computational time is large so 151x21 is chosen the convenient grid for producing the results of microchannel using nanofluids.

### 4.3.2 Validation with single phase approach numerical results

Grid size is 151x21,  $Al_2O_3$  water nanofluid with different Reynolds numbers

Table 4.2: code validation with single phase approach

Vol % and Re	$NU_{avg}$ kalteh et.al Experimental[23]	$NU_{avg}$ Present	$NU_{avg}$ Rajesh[24]
$Re = 285.86, 0.1\%$	7.7	7.87	7.6
$Re = 243.0, 0.2\%$	8.1	7.49	7.1

Here the two-phase approach numerical results is validated with single phase approach average

nusselt numbers at two different reynolds numbers,the numerical results of Rajesh and Venkatasubbaiah[24] validated with present results. At Reynolds number 285.86 with 0.1% volume concentration the present average nusselt number is close to [24] average nusselt number.

### 4.3.3 Effect of Reynolds number

The effect of reynolds number on the heat transfer at 0.1%, 0.2% volume concentrations  $Al_2O_3$  and water is continuous phase.

The figure 4.5, 4.6 is shows that as the Reynolds number increases heat transfer also increases.

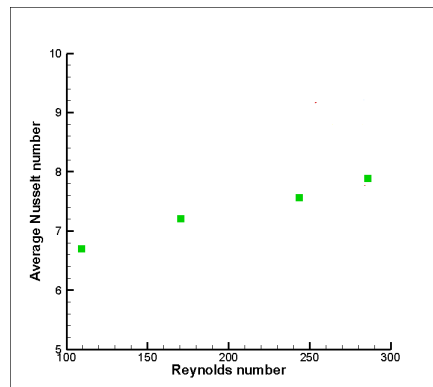


Figure 4.5:  $NU_{avg}$  vs  $RE$

The figure 4.5 represents the study about the effect of Reynolds number,the  $x$  axis is Reynolds number range from( $Re = 109.54$  to  $285.86$ ) and  $y$  axis represents the average nusselt number variation for each Reynolds number,and volume concentration is keeping constant means at same value i.e. at  $\phi=0.1\%$ . As the Reynolds number increases the inlet velocity will increase and this will create the fully developed flow very fast, due to this the heat carried by fluid will increases means convection will increases from the bottom wall of the channel hence the average nusselt is increases.

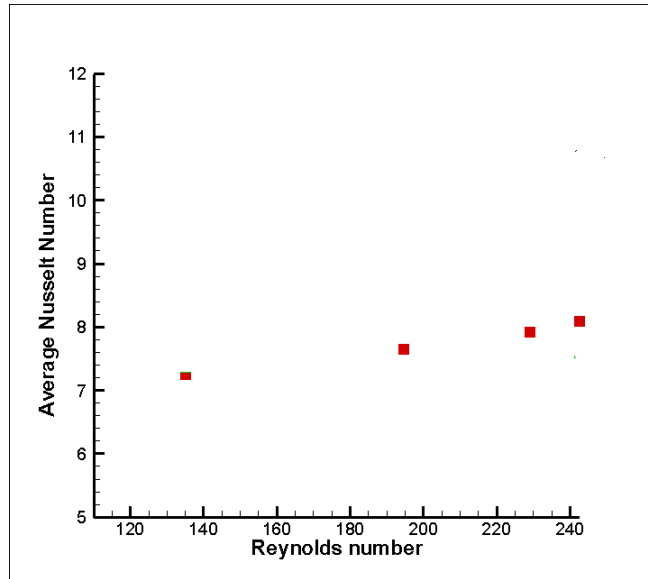


Figure 4.6:  $NU_{avg}$  vs  $RE$

The figure 4.6 also represents increase in heat transfer with increase of Reynolds at 0.2% volume fraction for the Re range from ( $Re = 140$  to  $240$ ), with increase in Reynolds number the fluid molecules will carry more heat from the wall with less time there by thermal boundary layer thickness gets reduced.

#### 4.3.4 effect of volume concentration

At Reynolds number  $Re = 243.2$ , for 0.1% and 0.2% volume concentrations observed the increment in heat transfer.

Table 4.3: average nusselt number variation with  $\phi$  %

0.1% volume concentration	0.2% volume concentration
$Re = 243.2$	$Re = 243.2$
$NU_{avg} = 7.489$	$NU_{avg} = 7.721$

This study is about the effect of volume fraction on heat transfer, at same Reynolds number ( $Re = 243.2$ ) as we increase the volume fraction from 0.1% to 0.2% the concentration of the particles i.e. volume density will increase due to this the thermal conductivity of nanofluid will increase hence the heat transfer increases.

### 4.3.5 effect of base fluids

The base fluids are water and kerosene, at  $Re = 400$ , with constant wall temperature condition, at the bottom wall of the channel temperature is 310K, the inlet temperature is 293K.

The  $Al_2O_3$  nano-particles dispersed into the above base fluids, the size of the particle is 40nm.

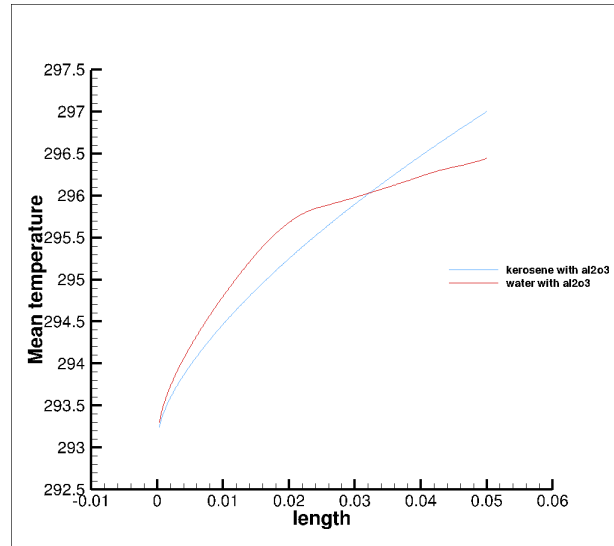


Figure 4.7: Length vs mean temperature

For both base fluids kerosene and water from the figure 4.7 the  $x$  axis represents the length of the channel and  $y$ -axis the mean temperature variation. The mean temperature for the water-based nanofluid is gradually increasing along the length of the channel whereas for kerosene-based nanofluid up to sudden length is gradual increases then fall down due to the effect of properties of kerosene nanofluid.

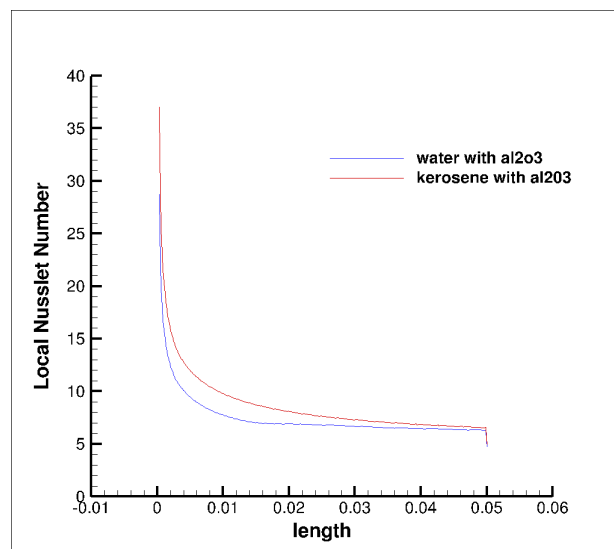


Figure 4.8: Length vs  $NU_{local}$

The figure 4.8 represents the variation of local nusselt number along the length of the channel for both water-based nanofluid as well as for kerosene-based nanofluid, the nusselt number at beginning of the length is more due to the temperature between fluid and wall is high as the length is increases this temperature difference is decreases hence the nusselt number will decrease. and velocity inlet for kerosene is more due to its properties as well as the Prandtl number also high for the kerosene compared to water. The table 4.4 represents the kerosene-based nanofluid will more heat transfer than the water-based nanofluid at same  $Re = 400$ ,  $\phi=1\%$ .

Table 4.4: average nusselt number variation with basefluids

Base fluid	Nano-particles	Re	$NU_{avg}$
water	$Al_2O_3(1\%)$	400	7.463
Kerosene	$Al_2O_3(1\%)$	400	8.690

The table 4.4 shows the effect of base fluids in heat transfer at same Reynolds number



## Chapter 5

# Results of impinging slot jet flow using nanofluids

An incompressible two-dimensional impinging slot jet laminar flow in a channel with using nanofluids with two-phase approach Eulerian-Eulerian model studied numerically. And observed that enhancement in heat transfer with the effect of Reynolds number( $Re$ ), volume concentrations, different aspect ratios, and different nanofluids.

### 5.1 Grid independence test

At  $Re=200$ , 0.1% volume concentration with water-aluminium oxide nanofluid, grids 440X120, 490X150, 560X175 showed the grid independence from velocity and temperature profiles.

The profiles are with half part of channel i.e right portion of the channel from the center of impingement to the outlet.

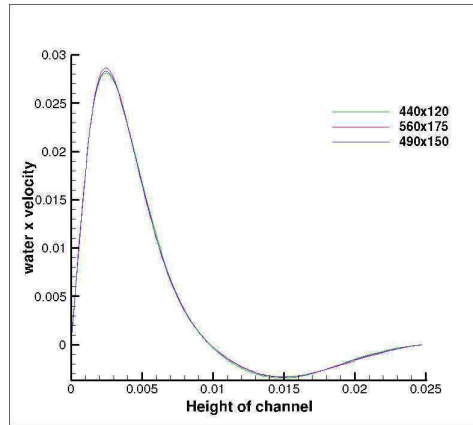


Figure 5.1: horizontal velocity of water L vs H

The figure 5.1 shows the horizontal velocity of water at Reynolds number( $Re = 200$ ) with volume fraction is 1%, the profile is plotted at  $x = 0.32$  which is near to the impinging zone. The velocity near to impinging zone is zero which satisfies no-slip boundary condition after that suddenly increases

due to hitting effect then falls down to zero, from this figure the velocity profiles are not changing with three different grids then grid independence done with velocity profile along with the height of the channel.

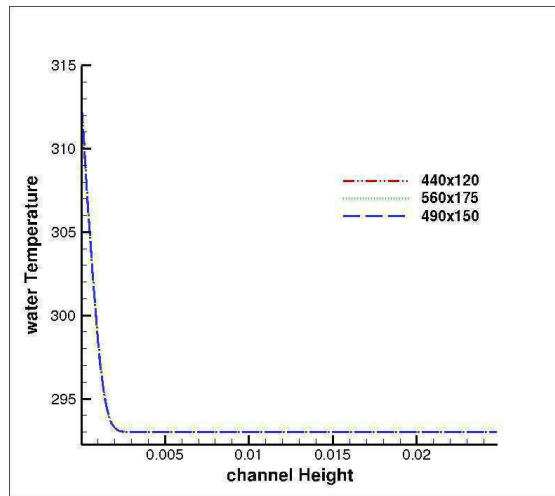


Figure 5.2: horizontal velocity of water L vs H

The variation of temperature profile of water along the height of the channel is given by figure 5.2 at the bottom wall temperature is maximum it will decrease as the height increases. From figures 5.1, 5.2 the velocity and temperature profiles are not showing any variation with respect to three different grids; it means grid independence has been achieved. Among these grids, 490X150 is chosen to save computational time.

## 5.2 Velocity and temperature contours at $Re = 200$

At  $Re = 200$ ,  $\phi = 1\%$ ,  $H/W = 4$  aspect ratio, water-aluminium oxide nanofluid. Inlet jet temperature is 293K, constant bottom wall temperature is 313K.

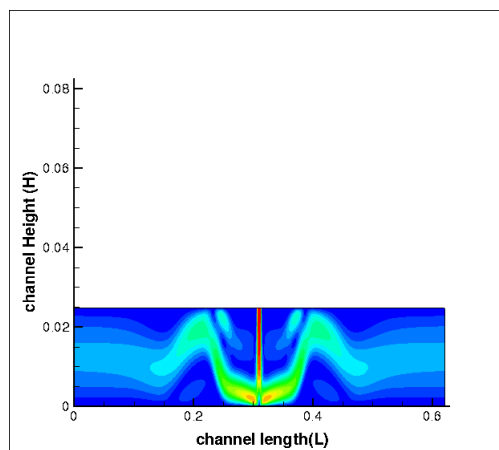


Figure 5.3: Velocity contour of water L vs H

From the figure 5.3 shows the variation of velocity of water jet through the length and height of the channel, the inlet velocity which is initialized vertically through a rectangular slot which is at the center of the channel. After the impingement of cold fluid molecules on to the targeted surface, their path will change both sides of the channel and velocity will become less. Here the velocity is maximum at the inlet of the slot after impingement it will decrease, the streamlines show that the path of flow after the impingement. And at the walls of the channel velocity is zero to satisfy no-slip boundary condition the equations 2.3.1, 2.3.2, 2.3.3 Eulerian-Eulerian equations for laminar case.

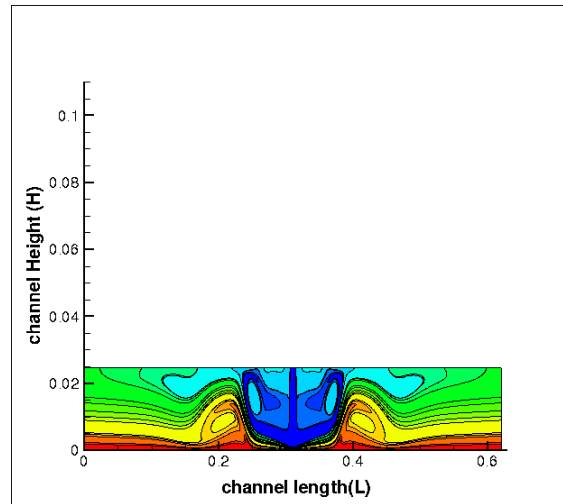


Figure 5.4: Temperature contour of water L vs H

The figure 5.4 shows the variation of temperature contour of water throughout the length and height of the channel. The bottom wall temperature is constant which is 313K, where the jet inlet temperature is 293K, this cold fluid molecules impinge on the targeted surface, from the figure we can see that the impinging zone became as cold fluid then their rate of heat transfer between wall and fluid is increased. The temperature getting changed from the stagnation zone to the outlet section of the channel which is shown by stream contours of temperature field.

### 5.3 Validation

Validation of solver with numerical results of lamraoui et.al [34]

At  $Re=200$ ,  $\phi =1\%$ ,  $Al_2O_3$  - water nanofluid and aspect ratio  $H/W = 4$ , particle size is 30 nm.

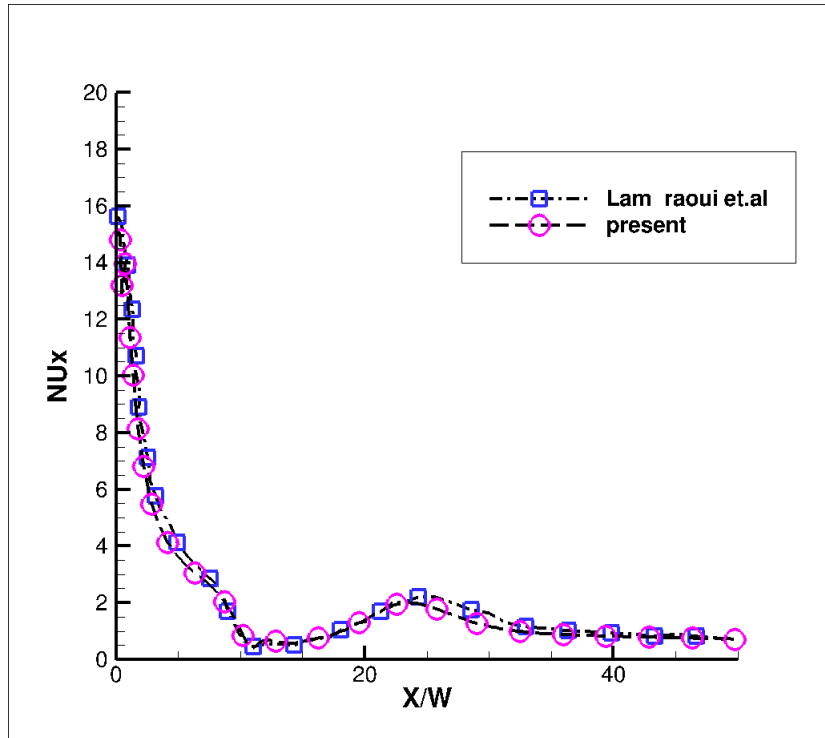


Figure 5.5: local nusselt number variation along L

The figure 5.5 shows the validation of present solver against [34] numerical results, the  $x$  axis represents non dimensional length and  $y$  is local nusselt number variation from impinging zone to right outlet section of the channel, at the impinging zone nusselt number is high due to more heat transfer between fluid and wall then gradually decreases again there is an increment in nusselt number due to effect of impingement.

The figure 5.6 shows the validation of present solver with [34, 35] numerical results at  $Re=100$ ,  $\phi = 1\%$ ,  $Al_2O_3$  - water nanofluid and aspect ratio  $H/W = 4$ , particle size is 30 nm.

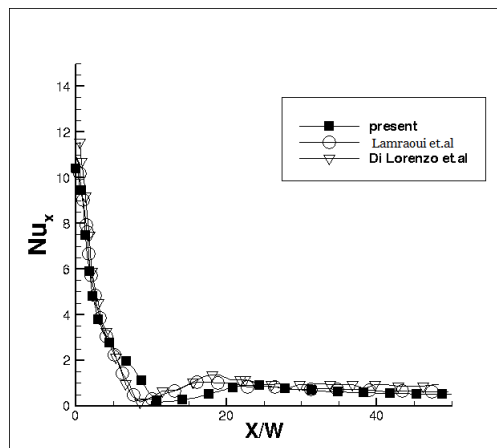


Figure 5.6: local nusselt number variation along L

The present solver local nusselt number variation along the length of the channel is very much matching with the numerical results of [34, 35], at  $Re=200,100$  with volume fraction is 1%.

## 5.4 Stream function contours of Dispersed phase(Aluminium oxide particles)

The impinging jet flow in a mini-channel with different Reynolds, The present below stream function contours are at three different Reynolds numbers with aluminium-oxide and water nano fluid, volume concentration taken is 2%, The aspect ratio( $H/W$ )=4 for all figures 5.7,5.8, 5.9.

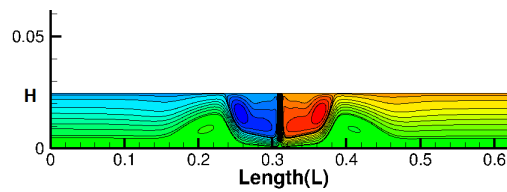


Figure 5.7: Stream function contour at  $Re=100$

From the above figure, we can observe that the stream function vortices are so close to the impingement zone then after some distance from the impingement zone the streamlines are becoming parallel.

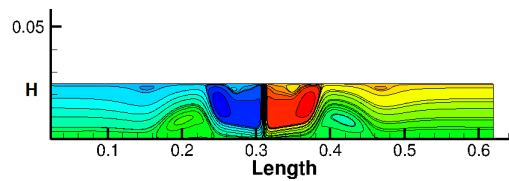


Figure 5.8: Stream function contour at  $Re=200$

From figure 5.8 the streamlines at  $Re=200$  the vortices are stretched and becomes large compared to  $Re=100$ .

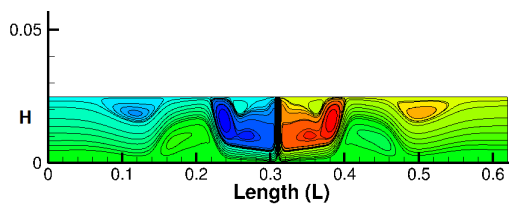


Figure 5.9: Stream function contour at  $Re=300$

The above figure shows that the large vortices are formed after the impingement, as the Reynolds becomes more hitting intensity of particles increases, the vortices will form little be away from the impinging zone.

## 5.5 Effect of Reynolds number

At  $\phi = 2\%$  , aspect ratio  $H/W = 4$ , particle size ( $d_p$ ) =30 nm.

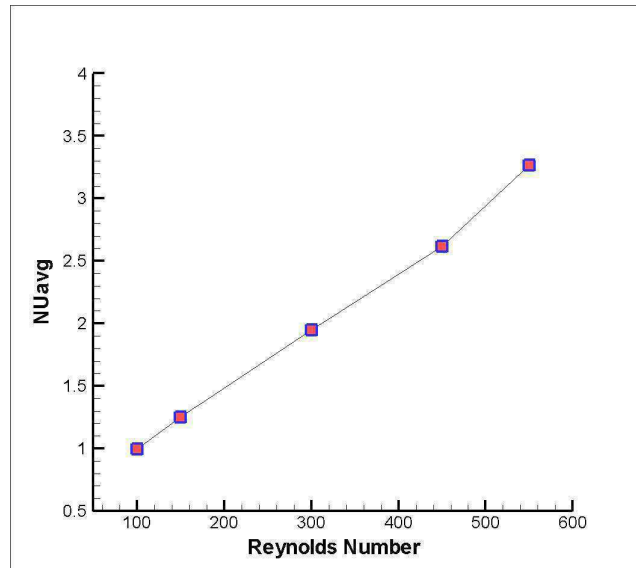


Figure 5.10:  $NU_{avg}$  with Reynolds number

from figure 5.10 we can say that as the Reynolds number varies from (Re=100 to 550) the average nusselt number increases from 0.99 to 3.49 it means the heat transfer increases. When the Reynolds number increases the jet inlet velocity increases due to this impingement intensity at the targeted surface is increases due to this heat transfer rate increases between nano fluid and wall.

## 5.6 Effect of volume concentration

At Re=200 with aspect ratio  $H/w = 4$

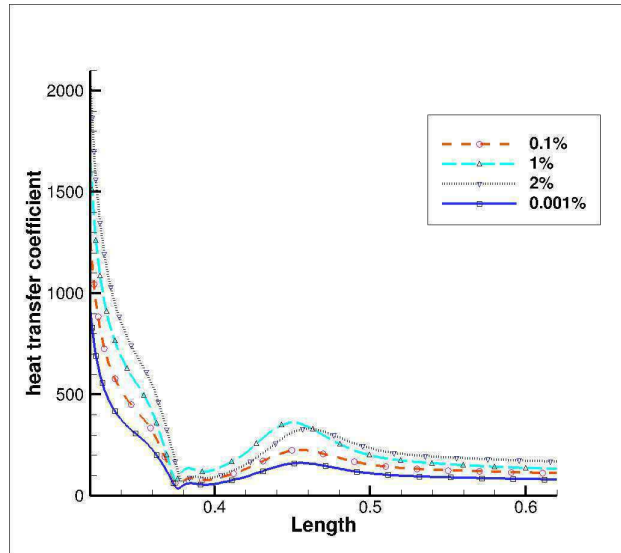


Figure 5.11: heat transfer coefficient along L

The figure 5.11 shows the variation of heat transfer coefficient from stagnation zone to right outlet section of the channel, as the volume fraction increases the nano-particles increases due to this the convection between base fluid and particle is increases overall thermal conductivity will increases there by heat transfer will increases.

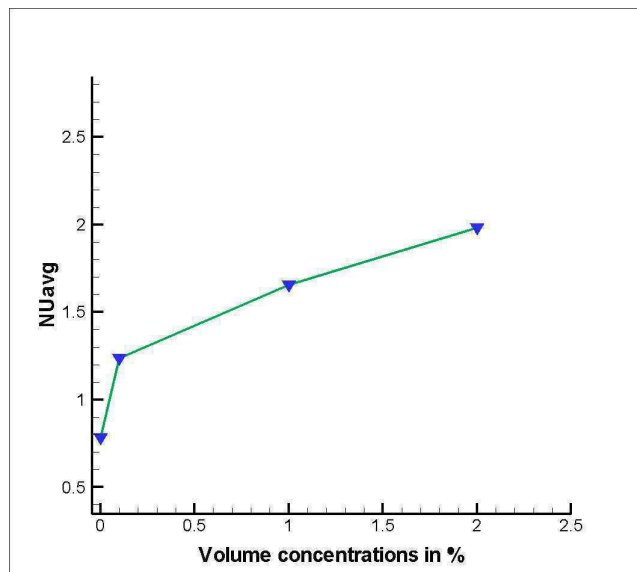


Figure 5.12:  $NU_{avg}$  vs  $\phi$

From above figure at the very low volume concentration(0.001%) the average nusselt number is 0.77 where as at 2%  $NU_{avg}$  is 1.99 from figure 5.12 shows that  $NU_{avg}$  increases with volume concentrations and the figure 5.11 shows that variation of heat transfer coefficient from jet impingement targeted surface zone to outlet of the section of the channel at different volume concentrations.

## 5.7 Effect of aspect ratio

At  $Re=200$ ,  $\phi = 0.1\%$ , for three aspect ratios 2,4,6.

Table 5.1: average nusselt number variation with aspect ratio

Reynolds number	Aspect ratio	$NU_{avg}$
Re=200	$H/W = 2$	2.183
Re=200	$H/W = 4$	1.654
Re=200	$H/W = 6$	1.257

From the table 5.1 at same Reynolds number as the aspect ratio( $H/W$ ) means jet inlet to targeted surface distance increases the average nusselt number decreases, due to the cold fluid molecules impinging intensity will decrease hence the rate of heat transfer between fluid and wall decreases.

## 5.8 Effect of nanofluids

At Reynolds number 200 with different nanofluids which are  $TiO_2$  -water,  $Al_2O_3$  -water,  $Cuo$  - water with  $\phi = 0.1\%$ , 1%, 2% and  $d_p$  is 30nm



Table 5.2: effect of nanofluids

Reynolds number	Type of nanofluid	$\phi = 0.1\%, NU_{avg}$	$\phi = 1\%, NU_{avg}$	$\phi = 2\%, NU_{avg}$
Re=200	water- $Al_2O_3$	1.2017	1.5246	1.7086
Re=200	water- $Cuo$	1.3218	1.7238	1.8237
Re=200	water- $Tio_2$	1.5820	1.8355	2.0013

The table 5.2 which shows the effect of different nanofluids on the heat transfer at  $Re = 200$  for different volume concentrations.

From the 5.2 at volume fractions 0.1%, 1%, 2% the average nusselt number is increases for three nanofluids but titanium oxide-water nanofluid showing more heat transfer than others due to the properties of  $Tio_2$ .

## 5.9 Velocity profiles of both phases at different locations

At  $Re = 200$ ,  $\phi=1\%$  the figure 5.13 shows the vertical velocity variations of both liquid and particles along the height of the channel, at the location  $x = L/2$ .

The vertical velocity at the wall is zero and as the height increases at inlet section this velocity is maximum for both water and Aluminium particles

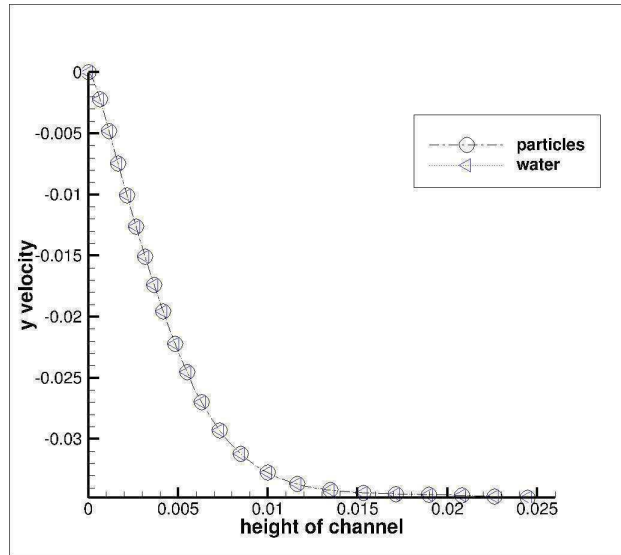


Figure 5.13: vertical inlet velocity along H

The figure 5.14 At  $Re = 200$  the horizontal velocity of both phases at location  $x=L/4$  the velocity profile is parabolic in nature, it shows that the velocity of both phases follows same profile with very negligible difference.

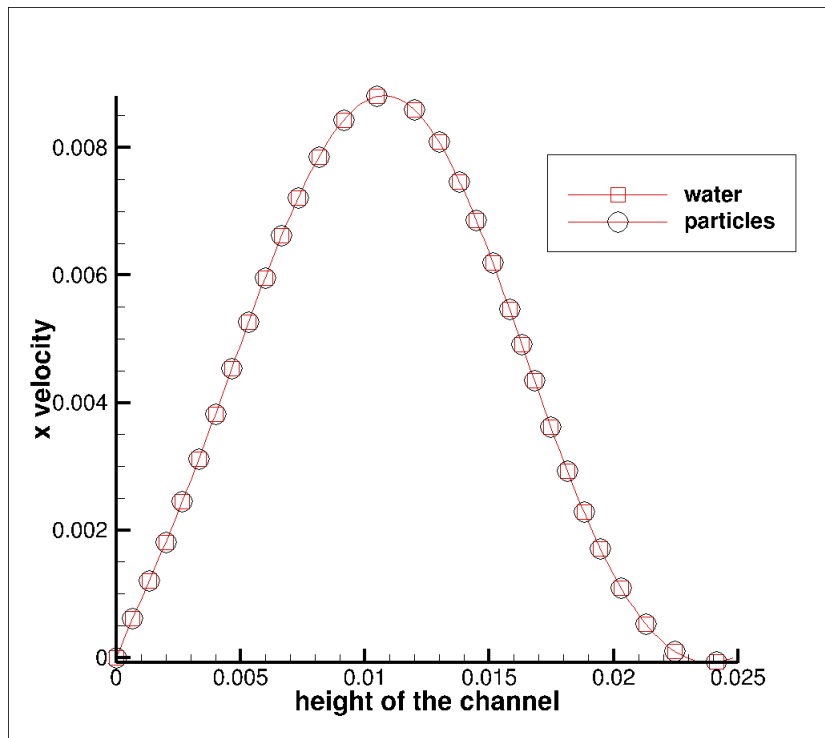


Figure 5.14: vertical velocity along Height of the channel

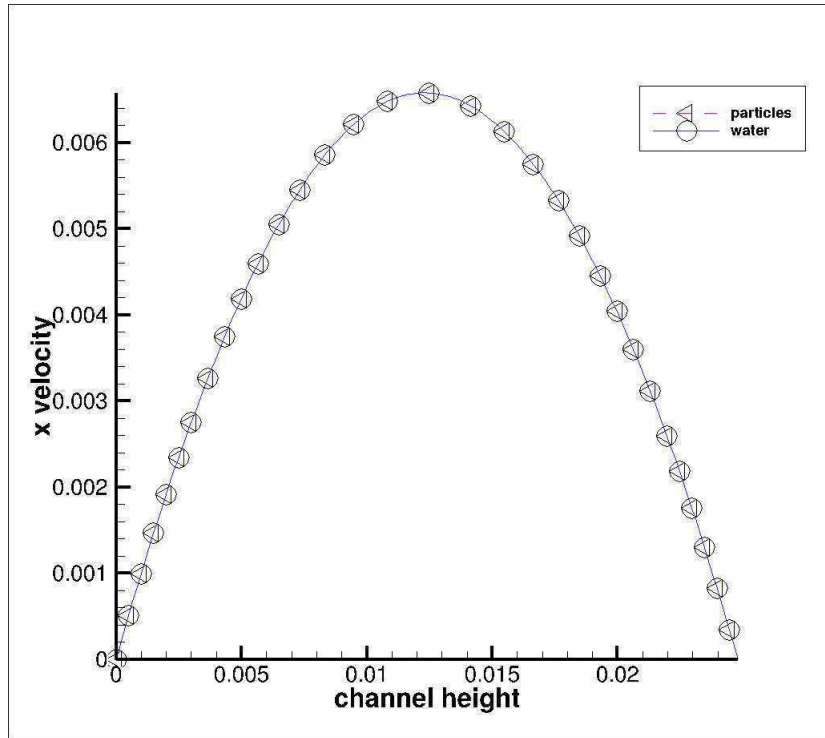


Figure 5.15: U velocity along Height of the channel

The figure 5.15 represents the horizontal velocity profile of both phases at outlet section of the channel i.e. at  $x=L$  variation from the bottom wall to top wall is pure parabolic and the velocity differences between both liquid and solid phases are almost negligible.

# Chapter 6

## Conclusions

Numerically have been studied an incompressible two dimensional laminar parallel flow through a microchannel using nanofluids, the impinging jet flow through a mini-channel using nanofluids by software OpenFOAM and ANSYS FLUENT. The following points are concluded from the simulations.

- Validated present solver against experimental[23] results.
- Studied that with the parallel flow in a microchannel, as the increase of Reynolds number from(109.54 to 285.86), heat transfer enhances by 17.63%.
- At  $Re = 243.2$  with parallel flow using  $Al_2O_3$ -water nanofluid, as the increment in particle concentration from(0.1% to 0.2%) heat transfer enhances by 3.01%.
- At  $Re = 400$ ,  $\phi=1\%$  The kerosene-based nanofluid has shown higher heat transfer than water-based nanofluid.
- Validated present solver against numerical results of [35, 34] at  $Re=200,100$  with impinging jet flow.
- Studied the effects of Reynolds number as  $Re$  increases from 100 to 550, heat transfer enhances by 223.23%
- At  $Re = 200$  with jet impingement as the increment in concentration from(0.001% to 0.1%) heat transfer enhances by by 71.4%
- Observed at  $Re = 200$  the effect of aspect ratios( $H/W = 2,4,6$ ) on the heat transfer that is as the aspect ratio increases average nusselt number decreases due to the impingement to target surface distance increases.
- Observed that at different locations the velocity differences between both the phases(liquid, solid) so small and negligible.
- Studied the effect of different nanofluids(water- $Al_2O_3$ ,water- $Cuo$ ,water- $TiO_2$ ),among these nanofluids at  $Re=200$ , volume fractions $\phi = 0.1\%$ ,  $1\%$ ,  $2\%$  at all volume fractions the  $TiO_2$ -water nanofluid has done better performance in heat transfer than other two nanofluids.

# References

- [1] S. Mokhatab, M. Fresky, and M. Islam. Application of Nanotechnology in Oil and Gas E&P. *JPT. Society of Petroleum Engineers* 18.
- [2] D. Wen, G. Lin, S. Vafaei, and K. Zhang. Review of nanofluids for heat transfer applications. *Particuology* 7, (2009) 141–150.
- [3] J. C. Maxwell. A treatise on electricity and magnetism, volume 1. Oxford: Clarendon Press, 1873.
- [4] S. U. Choi and J. A. Eastman. Enhancing thermal conductivity of fluids with nanoparticles. Technical Report, Argonne National Lab., IL (United States) 1995.
- [5] D. B. Tuckerman and R. F. W. Pease. High-performance heat sinking for VLSI. *IEEE Electron device letters* 2, (1981) 126–129.
- [6] O. Manca, P. Mesolella, S. Nardini, and D. Ricci. Numerical study of a confined slot impinging jet with nanofluids. *Nanoscale research letters* 6, (2011) 188.
- [7] J. Koo and C. Kleinstreuer. Laminar nanofluid flow in microheat-sinks. *International Journal of Heat and Mass Transfer* 48, (2005) 2652–2661.
- [8] D. Lelea, S. Nishio, and K. Takano. The experimental research on microtube heat transfer and fluid flow of distilled water. *International Journal of Heat and Mass Transfer* 47, (2004) 2817–2830.
- [9] S. P. Jang and S. U. Choi. Cooling performance of a microchannel heat sink with nanofluids. *Applied Thermal Engineering* 26, (2006) 2457–2463.
- [10] S. El Bécaye Maïga, C. Tam Nguyen, N. Galanis, G. Roy, T. Maré, and M. Coqueux. Heat transfer enhancement in turbulent tube flow using Al<sub>2</sub>O<sub>3</sub> nanoparticle suspension. *International Journal of Numerical Methods for Heat & Fluid Flow* 16, (2006) 275–292.
- [11] J. Li and C. Kleinstreuer. Thermal performance of nanofluid flow in microchannels. *International Journal of Heat and Fluid Flow* 29, (2008) 1221–1232.
- [12] A. K. Santra, S. Sen, and N. Chakraborty. Study of heat transfer due to laminar flow of copper–water nanofluid through two isothermally heated parallel plates. *International Journal of Thermal Sciences* 48, (2009) 391–400.

- [13] X. Wu, H. Wu, and P. Cheng. Pressure drop and heat transfer of Al<sub>2</sub>O<sub>3</sub>-H<sub>2</sub>O nanofluids through silicon microchannels. *Journal of micromechanics and microengineering* 19, (2009) 105,020.
- [14] V. Bianco, F. Chiacchio, O. Manca, and S. Nardini. Numerical investigation of nanofluids forced convection in circular tubes. *Applied Thermal Engineering* 29, (2009) 3632–3642.
- [15] R. Lotfi, Y. Saboohi, and A. Rashidi. Numerical study of forced convective heat transfer of nanofluids: comparison of different approaches. *International Communications in Heat and Mass Transfer* 37, (2010) 74–78.
- [16] M. H. Fard, M. N. Esfahany, and M. Talaie. Numerical study of convective heat transfer of nanofluids in a circular tube two-phase model versus single-phase model. *International Communications in Heat and Mass Transfer* 37, (2010) 91–97.
- [17] M. Kalteh, A. Abbassi, M. Saffar-Avval, and J. Harting. Eulerian–Eulerian two-phase numerical simulation of nanofluid laminar forced convection in a microchannel. *International journal of heat and fluid flow* 32, (2011) 107–116.
- [18] S. Z. Heris, S. G. Etemad, and M. N. Esfahany. Experimental investigation of oxide nanofluids laminar flow convective heat transfer. *International Communications in Heat and Mass Transfer* 33, (2006) 529–535.
- [19] S. Z. Heris, M. N. Esfahany, and S. G. Etemad. Experimental investigation of convective heat transfer of Al<sub>2</sub>O<sub>3</sub>/water nanofluid in circular tube. *International Journal of Heat and Fluid Flow* 28, (2007) 203–210.
- [20] M. Izadi, M. Shahmardan, M. Norouzi, A. Rashidi, and A. Behzadmehr. Cooling performance of a nanofluid flow in a heat sink microchannel with axial conduction effect. *Applied Physics A* 117, (2014) 1821–1833.
- [21] J.-Y. Jung, H.-S. Oh, and H.-Y. Kwak. Forced convective heat transfer of nanofluids in microchannels. In ASME 2006 International Mechanical Engineering Congress and Exposition. American Society of Mechanical Engineers, 2006 327–332.
- [22] M. Kalteh. Investigating the effect of various nanoparticle and base liquid types on the nanofluids heat and fluid flow in a microchannel. *Applied Mathematical Modelling* 37, (2013) 8600–8609.
- [23] M. Kalteh, A. Abbassi, M. Saffar-Avval, A. Frijns, A. Darhuber, and J. Harting. Experimental and numerical investigation of nanofluid forced convection inside a wide microchannel heat sink. *Applied Thermal Engineering* 36, (2012) 260–268.
- [24] R. Nimmagadda and K. Venkatasubbaiah. Conjugate heat transfer analysis of micro-channel using novel hybrid nanofluids (Al<sub>2</sub>O<sub>3</sub>+ Ag/Water). *European Journal of Mechanics-B/Fluids* 52, (2015) 19–27.
- [25] R. Nimmagadda and K. Venkatasubbaiah. Numerical Investigation on Conjugate Heat Transfer Performance of Microchannel Using Sphericity-Based Gold and Carbon Nanoparticles. *Heat Transfer Engineering* 38, (2017) 87–102.

- [26] R. Nimmagadda and K. Venkatasubbaiah. Experimental and multiphase analysis of nanofluids on the conjugate performance of micro-channel at low Reynolds numbers. *Heat and Mass Transfer* 53, (2017) 2099–2115.
- [27] M. Sarafraz, H. Arya, and M. Arjomandi. Thermal and hydraulic analysis of a rectangular microchannel with gallium-copper oxide nano-suspension. *Journal of Molecular Liquids* 263, (2018) 382–389.
- [28] A. J. Sundararaj, B. Pillai, and L. G. Asirvatham. Convective heat transfer analysis of refined kerosene with alumina particles for rocketry application. *Journal of Mechanical Science and Technology* 32, (2018) 1685–1691.
- [29] H. Lee, b. Yoon, and M. Ha. A numerical investigation on the fluid flow and heat transfer in the confined impinging slot jet in the low Reynolds number region for different channel heights. *International Journal of Heat and Mass Transfer* 51, (2008) 4055–4068.
- [30] D. Zhou and S.-J. Lee. Forced convective heat transfer with impinging rectangular jets. *International Journal of heat and mass transfer* 50, (2007) 1916–1926.
- [31] S. J. Palm, G. Roy, and C. T. Nguyen. Heat transfer enhancement with the use of nanofluids in radial flow cooling systems considering temperature-dependent properties. *Applied thermal engineering* 26, (2006) 2209–2218.
- [32] A. Kuznetsov and D. Nield. Natural convective boundary-layer flow of a nanofluid past a vertical plate. *International Journal of Thermal Sciences* 49, (2010) 243–247.
- [33] F. T. Dórea and M. J. De Lemos. Simulation of laminar impinging jet on a porous medium with a thermal non-equilibrium model. *International Journal of Heat and Mass Transfer* 53, (2010) 5089–5101.
- [34] H. Lamraoui, K. Mansouri, and R. Saci. Numerical investigation on fluid dynamic and thermal behavior of a non-Newtonian Al<sub>2</sub>O<sub>3</sub>–water nanofluid flow in a confined impinging slot jet. *Journal of Non-Newtonian Fluid Mechanics* 265, (2019) 11–27.
- [35] G. Di Lorenzo, O. Manca, S. Nardini, and D. Ricci. Numerical study of laminar confined impinging slot jets with nanofluids. *Advances in Mechanical Engineering* 4, (2012) 248,795.